JOURNAL OF VIROLOGY, Apr. 1981, p. 104-114
0022-538X/81/040104-11$02.00/0

Vol. 38, No. 1

# Map of Restriction Sites on Bacteriophage T4 Cytosine-Containing DNA for Endonucleases *Bam*HI, *Bgl*II, *Kpn*I, *Pvu*I, *Sal*I, and *Xba*I

ROBERT C. MARSH* AND MICHAEL L. HEPBURN

*Biology Program, University of Texas at Dallas, Richardson, Texas 75080*

Received 1 October 1980/Accepted 31 December 1980

A complete map of the cleavage sites of restriction endonucleases *Bam*HI, *Bgl*II, *Kpn*I, *Pvu*I, *Sal*I, and *Xba*I was determined for the cytosine-containing DNA of a bacteriophage T4 *alc* mutant. The 56 sequence-specific sites were assigned map coordinates based on a least-squares analysis of measured fragment lengths. Altogether, the lengths of 118 fragments from single and double enzyme digestions were measured by electrophoresis of the fragments in agarose gels. DNA fragments of known sequence or DNA fragments calibrated with fragments of known sequence were used as standards. The greatest deviation between an experimentally measured fragment length and its computed map coordinates was 3.0%; the average deviation was 0.8%. The total length of the wild-type T4 genome was calculated to be 166,200 base pairs.

Bacteriophage T4 is well characterized genetically; more than 100 genes have been identified on its 166-kilobase pair genome (23). As a result, the biochemistry of transcription and replication of T4 DNA has received considerable attention. Until recently however, further progress was hindered by the fact that the glucosylated hydroxymethylcytosine residues normally present in T4 DNA prevented restriction endonuclease analysis (6). This obstacle was surmounted when *alc* mutants of T4, which allow the growth and packaging of cytosine-containing DNA (dC-DNA), were isolated (16). Physical maps of cleavage sites now exist for restriction enzymes *Bam*HI, *Bgl*I, *Bgl*II, *Eco*RI, *Hin*dIII, *Kpn*I, *Pst*I, *Sal*I, *Sma*I, and *Xho*I (2, 3, 7, 12, 14, 22). These maps are circular due to the circular permutation of the base sequence within a population of linear T4 chromosomes.

In this report we present a unified computer-fitted map for the cleavage sites of *Bam*HI, *Bgl*II, *Kpn*I, and *Sal*I, all of which we mapped independently, and add to the T4 restriction map the cleavage sites of *Pvu*I and *Xba*I. *Pvu*I cleaves the dC-DNA of the *alc* mutant which we used at four sites within two regions on opposite sides of the circular restriction map. In effect, *Pvu*I cuts the T4 genome in half. *Xba*I cleaves at 23 sites to produce a set of moderately sized fragments, all but 3 of which are well separated upon electrophoresis in an agarose gel. In the accompanying report (24) these restriction maps are aligned with the T4 genetic map.

## MATERIALS AND METHODS

**Phage and bacterial strains.** Bacteriophage T4 *56*$^-$ (*am*E51 dCTPase$^-$) *den*A(nd28) *den*B(Δ*r*IIH23B) *alc*8 and its restriction/modification-negative hosts *Escherichia coli* K803 (*supE hsdS rgl gal met*) and B834 (*supE*$^+$ $r_B^-$ $m_B^-$ *gal met*) were provided by L. Snyder (16). The triple-mutant parent for the *alc* mutant was constructed by R. Bruner and was thought to carry the 4.2-kilobase (kb) *r*II deletion H23, which spans the *r*IIA and *r*IIB cistrons and extends into *den*B. However, heteroduplex analysis and sensitivity to acriflavin have shown that the *r*II deletion carried by these mutants is considerably longer and extends to the *ac* locus (9). By electron microscopy of heteroduplexes, we measured the *r*IIH23 deletion of Bruner to be 5.8 kb long, with its terminus at the left end of the *r*IIA gene indistinguishable from the terminus for the *r*IIH23 deletion (8). We refer to this deletion as *r*IIH23B. T4 *αgt*8 *βgt*10 and *E. coli* U95 *rgl* (5), which lacks UDP-glucose pyrophosphorylase, were obtained from N. Sinha.

**Growth of bacteriophage and isolation of DNA.** To obtain T4 particles containing dC-DNA, the T4 *alc* quadruple mutant was grown first in *E. coli* K803 and then in *E. coli* B834 as described by Snyder et al. (16), except that H broth was used instead of M9S medium. H broth contains (per liter) 8 g of nutrient broth (Difco Laboratories), 5 g of peptone (Difco), 5 g of NaCl, and 1 g of glucose. Particles with nonglucosylated hydroxymethylcytosine-containing DNA were obtained by growing the T4 glucosyl transferase mutant in *E. coli* U95 *rgl*. Phage particles were purified by differential centrifugation and then suspended in 20 mM Tris-hydrochloride (pH 7.8)–0.5 mM EDTA.

For isolation of DNA, 0.1 volume of 10% sodium

dodecyl sulfate was added to the phage, and the suspension was heated to 65°C for 5 min to disrupt the particles. The solution of T4 dC-DNA was extracted several times with water-saturated phenol, dialyzed against 20 mM Tris-hydrochloride (pH 7.8)–0.5 mM EDTA, and stored at −20°C.

**Restriction endonuclease digestion.** Restriction endonucleases were purchased from New England Biolabs. A standard reaction mixture was used for all digestions and contained 20 mM Tris-hydrochloride (pH 7.8), 10 mM $MgCl_2$, 10 mM NaCl, 7 mM 2-mercaptoethanol, 0.2 mM EDTA, and 0.1% gelatin or 0.01% bovine serum albumin (Bethesda Research Laboratories). Sufficient enzyme was added to give complete digestion within a 6-h incubation at 37°C. When the DNA was digested with more than one enzyme, all enzymes were added at the beginning of the digestion period.

For secondary cleavage of restriction fragments, either fragments purified from preparative agarose gels or bands cut from ethidium bromide-stained 0.6% low-melting-point agarose gels were used. For purification of fragments, the agarose gel was dissolved with KI at 37°C, and the DNA was bound selectively to a short column of hydroxylapatite (Bio-Gel HT; Bio-Rad Laboratories). The DNA was eluted with 0.5 M sodium phosphate buffer (pH 6.8) and banded in a KI density gradient (1). The isopycnic centrifugation in KI was necessary to consistently obtain DNA readily cleavable with small amounts of restriction endonucleases. With the second technique, the excised pieces of gel were soaked for 1 h in water to reduce the amount of ethidium bromide, melted at 65°C, and placed in the bovine serum albumin-containing reaction mixture (10).

**Gel electrophoresis.** DNA digests were fractionated by electrophoresis on 18-cm slab gels of 0.5 or 1.2% agarose (SeaKem; FMC Corp.) or 0.6% low-melting-point agarose (Bethesda Research Laboratories) in an apparatus constructed by the method of Sugden et al. (18). The gels contained 20% glycerol and 80 mM Tris-maleate (pH 7.8). The running buffer was 40 mM Tris-maleate (pH 7.8). Up to 300 μl of the DNA digest, adjusted to contain 10% sucrose, was placed in each well, and 30 to 50 V was applied for 16 h at room temperature. DNA was visualized by immersing the gel in a solution containing 5 μg of ethidium bromide per ml for 15 min and destaining in water for 15 min, followed by short-wave UV illumination. Photographs were taken by using Polaroid type 55 P/N film and an orange Wratten 23A filter (Eastman Kodak).

**Molecular weight standards and fragment size measurement.** The sizes of T4 restriction fragments were determined from their electrophoretic mobilities relative to lambda phage DNA (λcI *ts*857 *S*7; obtained from E. Burgi) and its *Eco*RI fragments and relative to the *Alu*I, *Eco*RI, and *Hin*cIII fragments of plasmid pBR322 DNA (obtained from H. Boyer in *E. coli* RR1). The recently revised values of 49.13, 21.57, 7.54, 5.90, 5.68, 4.84, and 3.60 kb were assumed for lambda DNA and its six *Eco*RI fragments (4). The sizes of the pBR322 fragments are known from the nucleotide sequence of pBR322 DNA (19). These fragments provide a set of well-spaced standards which extends down to 11 base pairs (bp).

The distances of migration of the standards in the gel were plotted *versus* the logs of their lengths. Within the central, linear portion of the curve, a best-fit line was determined by the least-squares method. At the nonlinear ends of the plot, the values were connected to yield a continuous curve. The lengths of the unknown fragments less than 20 kb long were read directly from the plot and, in the nonlinear portions of the curve, were bracketed closely by standard values, The lengths of fragments more than 20 kb long were determined by summing subfragment lengths.

During construction of the unified restriction map, the measured fragment lengths were adjusted by the mapping program of Schroeder and Blattner (15) to minimize the sum of the squares of the fractional deviations between the measured lengths and the lengths predicted by the map coordinates. It is these adjusted values that are used throughout this report, unless otherwise noted.

## RESULTS

**Basis for construction of a *Bgl*II-*Xba*I cleavage map of T4 dC-DNA.** The restriction endonucleases *Bam*HI, *Bgl*II, *Hpa*I, *Kpn*I, *Pvu*I, *Pvu*II, *Sac*I, *Sal*I, *Sma*I, *Xho*I, and *Xba*I were each tested in an attempt to identify one or more nucleases that cleave the dC-DNA of T4 *am*E51 *den*A *den*B(Δ*r*IIH23B) *alc*8 to produce sets of 15 to 20 moderately sized fragments, each of which can be well resolved by gel electrophoresis. It was anticipated that such sets would simplify the initial mapping of restriction sites, and, more importantly, would be useful for future studies (e.g., by facilitating Southern blot hybridization analyses). *Xba*I came closest to meeting the criteria; it produced 23 fragments that were resolved into 21 well-separated bands in a 0.5% agarose gel (Fig. 1). The largest fragment was 17.9 kb long, and only band 2 contained more than one DNA fragment (it contained three fragments). Next best was *Bgl*II, with 13 fragments and 10 bands, three of which were composed of overlapping or closely migrating pairs of fragments (Fig. 1). Unfortunately, the largest *Bgl*II fragment was 55.8 kb long, representing about one-third of the T4 genome.

To construct a map of the *Bgl*II and *Xba*I cleavage sites on T4 dC-DNA, the DNAs from individual bands were subjected to reciprocal digestion; i.e., the *Bgl*II fragment or fragments in each band were digested with *Xba*I and vice versa. *Bgl*II and *Xba*I fragments that overlapped on the T4 genome would yield one *Bgl*II-*Xba*I subfragment in common, and on this basis, overlaps could be identified. By proceeding from overlap to overlap, an outline of the cleavage map was drawn. To complete the map, we positioned *Bgl*II and *Xba*I fragments which were fully contained within larger *Xba*I or *Bgl*II fragments and thus not cleaved in the reciprocal digestions. These fragments are referred to as

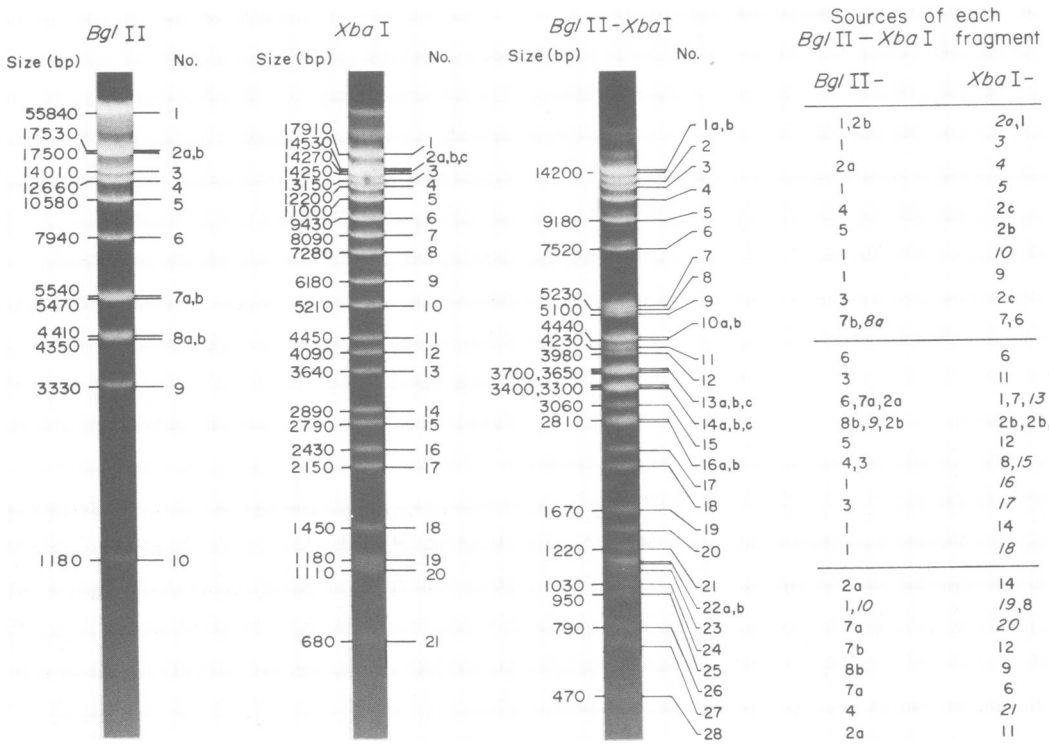


FIG. 1. *Restriction fragments produced by cleavage of T4 alc mutant dC-DNA with BglII and XbaI individually and in combination. The fragments were electrophoresed in an 0.6% agarose gel and visualized by ethidium bromide staining. Each fragment from the single and double digestions is numbered in order of decreasing size. An additional letter designates overlapping fragments. Minor bands that are unlabeled in this and the following figures represent DNA which was digested incompletely, perhaps due to the presence of a few hydroxymethylcytosine residues. The size given for each fragment is an adjusted value calculated during construction of the unified map (Fig. 2), which contains, in addition to the BglII and XbaI sites, the cleavage sites of BamHI, KpnI, PvuI, and SalI. The values are based on a least-squares analysis designed to minimize the fractional deviation between measured and predicted lengths, as described in the text. For the 55.8-kb fragment, the value represents the sum of subfragment lengths. The table at the right lists the individual BglII and XbaI fragments from which each subfragment in the double digestion could be derived. This was determined by isolating the individual BglII and XbaI fragments and then digesting them with XbaI and BglII, respectively. Italicized numbers indicate fragments not cleaved by the secondary digestion. These are internal subfragments of larger BglII and XbaI primary fragments.*

internal subfragments to distinguish them from the overlapping terminal subfragments. Their initial assignments on the map were based on their presence among the subfragments of a larger fragment. When two or more internal subfragments were present, these subfragments were ordered by examining the products of a partial digestion of the larger fragments, or other restriction enzymes were used to divide the larger fragments into smaller segments for analysis.

In the four cases where DNA bands contained more than one fragment (viz., *Bgl*II-2, -7, and -8 and *Xba*I-2), the subfragments which were produced by the reciprocal digestions had to be assigned to specific fragments for mapping. Restriction endonuclease *Pvu*I was found to cleave *Bgl*II-2a but not *Bgl*II-2b. Therefore, *Pvu*I was used to separate *Bgl*II-2a from *Bgl*II-2b, which was then cleaved with *Xba*I to determine its *Xba*I subfragments. Similarly, *Bgl*II-7b was separated from *Bgl*II-7a by selectively cleaving *Bgl*II-7a with *Xho*I. *Bgl*II-7b was then cleaved with *Xba*I for subfragment determination. With *Bgl*II-8, only one of the two fragments was cleaved by *Xba*I, making the assignment of subfragments straightforward. With the *Xba*I-2 triplet, *Xba*I-2a was not cleaved by *Bgl*II; the two remaining fragments were separated by selectively cleaving *Xba*I-2b with *Pvu*I. *Xba*I-2c was then cleaved with *Bgl*II to determine its subfragments.

In Fig. 1, all *Bgl*II-*Xba*I subfragments are displayed in an agarose gel of a *Bgl*II-*Xba*I double digest of the T4 dC-DNA. At the side of the gel are listed the individual *Bgl*II and *Xba*I fragments from which each *Bgl*II-*Xba*I subfragment could be derived by reciprocal digestion. The internal subfragments which were not cleaved by reciprocal digestion are italicized.

In Table 1, the *Bgl*II-*Xba*I subfragments are grouped to form a matrix that can be read horizontally for the subfragment composition of each of the *Xba*I fragments and vertically for the subfragment composition of each of the *Bgl*II fragments. Internal subfragments are indicated by a *b* superscript. In this table only subfragment sizes are listed for the sake of clarity.

An outline of the *Bgl*II-*Xba*I map of T4 dC-DNA can be read directly from Table 1 by starting with a subfragment derived from an overlap between a *Bgl*II fragment and an *Xba*I fragment. For example, this can be done with the 41,200-bp subfragment of *Xba*I-1 and *Bgl*II-2b in the upper left corner of the table. Scanning vertically, the subfragment from the other end of the *Bgl*II-2b fragment is noted. This is the 3,300-bp subfragment overlapping *Xba*I-8. Thus, *Xba*I-1 can be juxtaposed with *Xba*I-8 on the map. The other end of *Xba*I-8 is found by scanning horizontally, and the *Bgl*II fragment with which it overlaps is noted. By continuing to trace the *Bgl*II and *Xba*I fragments alternately, a circular map of the ends of the fragments can be deduced.

For the 13 *Bgl*II fragments, the resulting map is complete, since no *Xba*I fragment contained more than one internal subfragment when cleaved by *Bgl*II. This map is shown in Fig. 2. Also shown is the *Xba*I cleavage mpa, which was completed by ordering the *Xba*I fragments that fell within *Bgl*II fragments 1, 2a, and 3, as described below.

**Ordering of internal fragments to complete the *Xba*I cleavage map.** The neighboring *Bgl*II fragments 2a and 3 contain two internal *Xba*I fragments each (*Xba*I-4 and -13 and *Xba*I-15 and -17, respectively). To order these internal fragments on the map, *Bgl*II-2a and -3 were partially digested with *Xba*I. Based on direct size measurements, unadjusted during map construction, *Bgl*II-2a yielded a 5.00-kb partial product, which corresponded to the 4.87-kb sum (4.88 kb, unadjusted) of the lengths of *Xba*I-13 and the end of *Xba*I-14 that overlapped *Bgl*II-2a. With *Bgl*II-3, 6.36- and 7.88-kb partial products were measured; the first of these corresponded to the 6.12-kb sum (6.24 kb, unad-

TABLE 1. *Subfragments produced by reciprocal digestion of individual BglII and XbaI fragments*[a]

| *Xba*I fragment | Size (bp) of *Bgl*II fragment: | | | | | | | | | | | | |
|---|---|---|---|---|---|---|---|---|---|---|---|---|---|
| | 1 | 2a | 2b | 3 | 4 | 5 | 6 | 7a | 7b | 8a | 8b | 9 | 10 |
| 1 | | | 14,200 | | | | 3,700 | | | | | | |
| 2a | 14,530[b] | | | | | | | | | | | | |
| 2b | | | | | | 7,520 | | | | | 3,400 | 3,330[b] | |
| 2c | | | | 5,100 | 9,180 | | | | | | | | |
| 3 | 13,150[b] | | | | | | | | | | | | |
| 4 | | 12,200[b] | | | | | | | | | | | |
| 5 | 11,000[b] | | | | | | | | | | | | |
| 6 | | | | | | | 4,230 | 790 | | 4,410[b] | | | |
| 7 | | | | | | | | 3,650 | 4,440 | | | | |
| 8 | | | 3,300 | | 2,810 | | | | | | | | 1,180[b] |
| 9 | 5,230 | | | | | | | | | | 950 | | |
| 10 | 5,210[b] | | | | | | | | | | | | |
| 11 | | 470 | | 3,980 | | | | | | | | | |
| 12 | | | | | | 3,060 | | | 1,030 | | | | |
| 13 | | 3,640[b] | | | | | | | | | | | |
| 14 | 1,670 | 1,220 | | | | | | | | | | | |
| 15 | | | | 2,790[b] | | | | | | | | | |
| 16 | 2,430[b] | | | | | | | | | | | | |
| 17 | | | | 2,150[b] | | | | | | | | | |
| 18 | 1,450[b] | | | | | | | | | | | | |
| 19 | 1,180[b] | | | | | | | | | | | | |
| 20 | | | | | | | | 1,110[b] | | | | | |
| 21 | | | | | 680[b] | | | | | | | | |

[a] Individual *Bgl*II and *Xba*I fragments were redigested with *Xba*I and *Bgl*II, respectively. The sizes of the resulting subfragments are given.

[b] Internal subfragments, which represented entire *Bgl*II or *Xba*I fragments contained within the larger primary fragments.

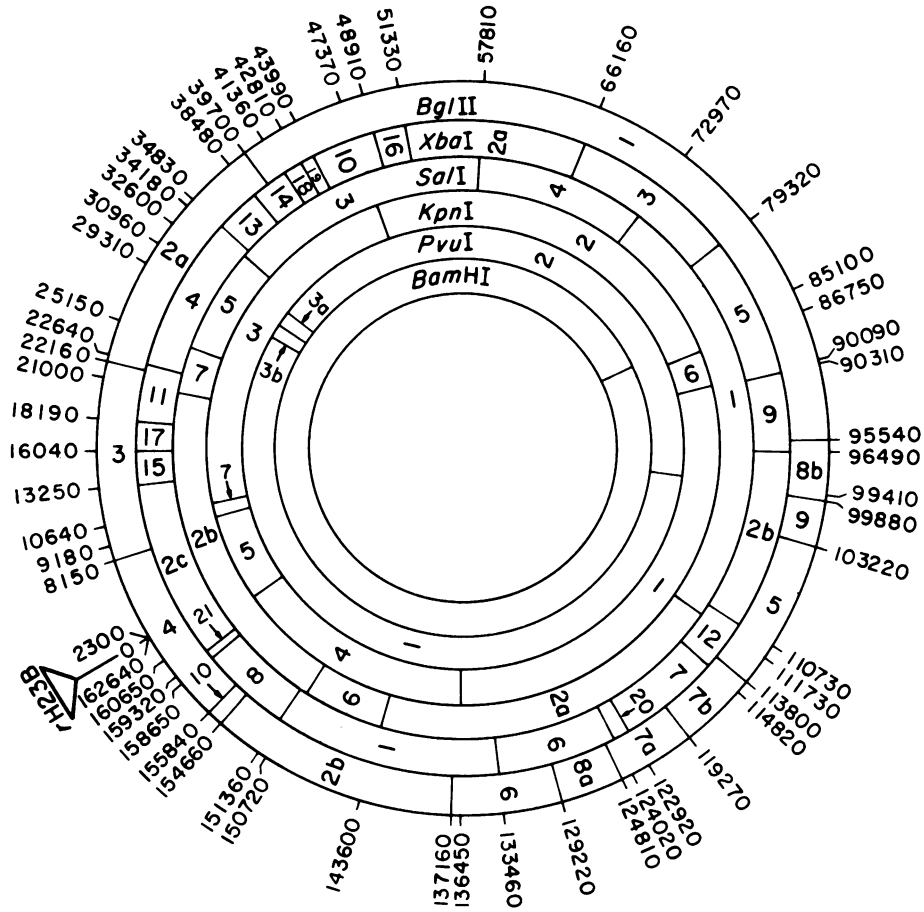


FIG. 2. *Map of cleavage sites on T4 alc mutant dC-DNA for restriction endonucleases BamHI, BglII, KpnI, PvuI, SalI, and XbaI. Coordinates (in base pairs) for the cleavage sites are listed around the outside of the map. They were determined by using the computer mapping program of Schroeder and Blattner (15), as described in the text. The coordinates are those expected with T4 DNA carrying no deletions and containing 166,200 bp. The 5.8-kb rIIH23B deletion carried by T4 alc mutant DNA, which was used to construct the restriction map, removes the standard zero point on the map at the juncture between the rIIA and B cistrons. The position of the deletion 5,850 bp from BglII-3 is based on the heteroduplex mapping described in the accompanying paper (24). In that study, the average measured distance from the deletion to BglII-3 was 5,720 bp. Here, this value was adjusted to 5,850 bp to correct for the 2.3% difference which existed between the length of BglII-4 measured in the heteroduplex analysis and the BglII-4 length determined by agarose gel electrophoresis. A coordinate of 2,300 bp was assigned to the left terminus of the deletion located at the end of the rIIA cistron from a size estimate of the cistron based on a heteroduplex analysis (8).*

justed) of the lengths of *Xba*-I-17 and the end of *Xba*I-11 that overlapped *Bgl*II-3, and the second corresponded to the 7.89-kb sum (7.93 kb, unadjusted) of the lengths of *Xba*I-15 and the end of *Xba*I-2c that overlapped *Bgl*II-3. Thus, we concluded that the overall map order is *Xba*I-14, -13, -4, -11, -17, -15, -2c, as shown on the map in Fig. 2.

For *Bgl*II-1, which contained seven internal *Xba*I fragments, partial digestion with *Xba*I provided insufficient data to order these fragments. Therefore, *Sal*I and *Kpn*I were used to cut *Bgl*II-1 into smaller segments for analysis.

To orient the *Sal*I and *Kpn*I segments of *Bgl*II-1 relative to the rest of the *Bgl*II-*Xba*I map, a complete map of the *Sal*I and *Kpn*I sites on the T4 *alc* mutant dC-DNA was constructed. Each *Bgl*II and *Xba*I fragment was digested with *Sal*I, and the products were analyzed on agarose gels. The same was done with *Kpn*I. Figures 3 and 4 shows individual *Sal*I and *Kpn*I digests and double digests of these enzymes with *Bgl*II and *Xba*I. The subfragments from the double digests are labeled first as to the *Bgl*II or *Xba*I fragment from which each subfragment was derived; after the hyphen is the number of

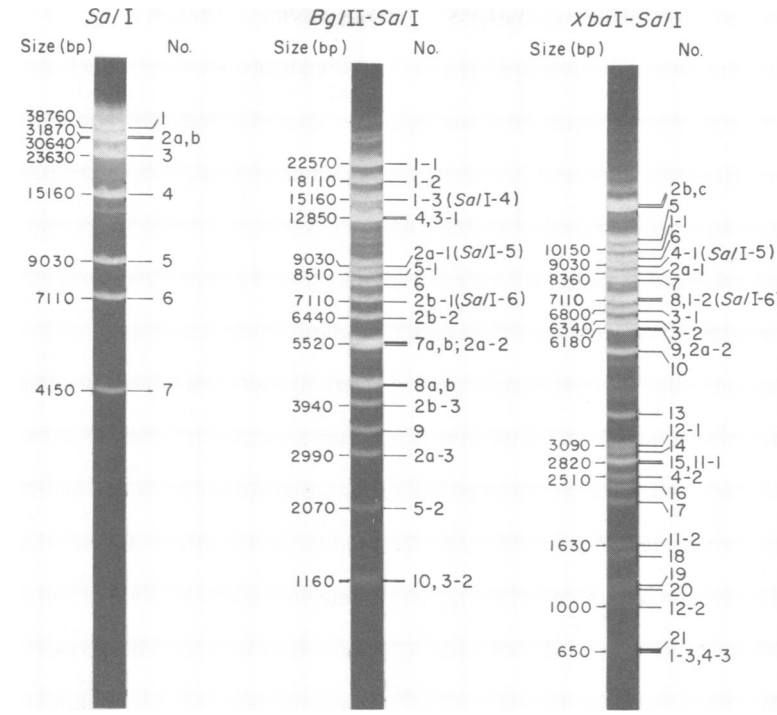


FIG. 3. *Agarose gel electrophoresis of the restriction fragments produced by cleavage of T4 alc mutant dC-DNA with SalI alone and with SalI in combination with BglII and XbaI. Fragment sizes were determined as described in the legend to Fig. 1; when greater than 20 kb, these sizes represent sums of subfragment lengths. For the double digestions, sizes are listed only if the fragment resulted from a secondary cleavage of a BglII or XbaI fragment by SalI. Each of these subfragments is labeled according to the BglII or XbaI fragment from which it was derived, followed by a number to designate the particular subfragment.*

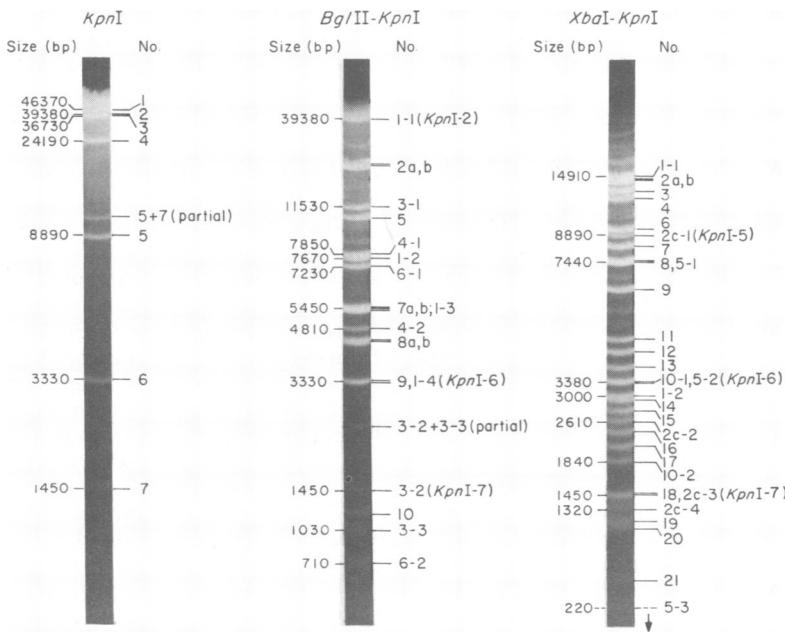


FIG. 4. *Agarose gel electrophoresis of restriction fragments produced by cleavage of T4 alc mutant dC-DNA with KpnI alone and with kpnI in combination with BglII and XbaI. Fragment sizes were determined and subfragments were numbered as described in the legends to Fig. 1 and 3.*

the particular subfragment. For example, in the *Bgl*II-*Sal*I digest in Fig. 3, the bands labeled 1-1, 1-2, and 1-3 represent the three subfragments derived from *Bgl*II-1 by *Sal*I cleavage. Because the locations of all *Bgl*II sites and *Xba*I sites outside *Bgl*II-1 were known, the results permitted the *Sal*I and *Kpn*I sites outside *Bgl*II-1 to be assigned unambigously. For example, Fig. 3 shows that *Sal*I cut *Bgl*II-5, yielding 8,510- and 2,070-bp subfragments and that it cut *Xba*I-12, which overlapped *Bgl*II-5, yielding 3,090- and 1,000-bp subfragments. These subfragments could be produced (Fig. 2) only if the *Sal*I cleavage site was located 2,070 bp from the end of *Bgl*II-5 which overlapped *Xba*I-12 (i.e., proximal to *Bgl*II-7b).

Assignment of all *Sal*I sites outside *Bgl*II-1 left only the sites which yielded *Sal*I fragments 1, 3, and 4 to be ascertained. With *Bgl*II-1, *Sal*I cut at two sites, producing 22,570- and 18,110-bp terminal fragments and an internal fragment which corresponded to the 15,160-bp *Sal*I-4 fragment. A 23,630-bp fragment the size of *Sal*I-3 would have resulted if the 18,110-bp terminal subfragment of *Bgl*I-1 were positioned next to the 5,520-bp terminal fragment of *Bgl*II-2a, and in this orientation, *Sal*I-1 could be accounted for by the other end of *Bgl*I-1, together with adjoining subfragments.

*Kpn*I cleaved *Bgl*II-1 into four subfragments; the internal subfragments corresponded to *Kpn*I-2 and -6, and the terminal subfragments were 5,450 and 7,670 bp long. *Kpn*I-6 was placed next to the 5,450-bp terminal subfragment on the basis of a partial *Kpn*I digestion of *Bgl*II-1. This fixed the positions of the other two subfragments. To orient the resulting *Kpn*I map of *Bgl*II-1 with respect to the *Kpn*I sites outside *Bgl*II-1, the *Kpn*I cleavage products of *Sal*I-3 were examined. Only one *Kpn*I cleavage site was present in *Sal*I-3 (data not shown). This was possible only if the end of *Bgl*II-1 which contained *Kpn*I-6 was located distal to *Sal*I-3. Thus, the 7,670-bp terminal *Kpn*I subfragment of *Bgl*II-1 was placed adjacent to *Bgl*II-2a, and the 5,450-bp other terminal *Kpn*I subfragment was placed along with *Kpn*I-6 at the end of *Bgl*II-1 next to *Bgl*II-8b.

After the positions of all *Sal*I and *Kpn*I subfragments within *Bgl*II-1 were established, all of the *Xba*I cleavage sites within this region except the site between the neighboring small fragments *Xba*I-18 and -19 could be assigned unambiguously, based on an analysis of the *Sal*I and *Kpn*I cleavage products of each of the *Xba*I fragments that fell within or overlapped *Bgl*II-1. As Fig. 4 shows, *Kpn*I-6 was cleaved from *Xba*I-5. This placed *Xba*I-5 adjacent to *Xba*I-9 at the clockwise end of *Bgl*II-1 in Fig. 2. Next, *Xba*I-3 and -2a were cleaved by *Sal*I to produce the 6,340-, 6,800-, 8,360-, and 6,180-bp fragments (Fig. 3) expected if *Xba*I-3 and -2a were positioned after *Xba*I-5, as shown in Fig. 2. Figure 4 shows that *Xba*I-10 was cut with *Kpn*I to produce 3,380- and 1,840-bp fragments. Placement of the shorter fragment proximal to *Xba*I-2a left room for a fragment the size of *Xba*I-16, whereas the space between *Xba*I-10 and -14 could accommodate *Xba*I-18 and -19.

The orientation of *Xba*I-18 and -19 relative to *Xba*I-10 was ascertained by examining an *Xba*I digestion of nonglucosylated hydroxylmethylcytosine-containing T4 DNA isolated from an α- and β-glucosyl transferase mutant of T4. Although resistant to most restriction enzymes, this DNA is cleaved by *Xba*I, although not as readily as dC-DNA. We observed that *Xba*I rarely cleaved the recognition site at the counterclockwise end of *Xba*I-10, so that in an agarose gel *Xba*I-10 and -19 were replaced by a larger fragment, which corresponded in size to the sum of the lengths of these fragments. *Xba*I-18 was present in a normal amount. This placed *Xba*I-19 adjacent to *Xba*I-10, as shown in Fig. 2.

**Location of the *Pvu*I and *Bam*HI cleavage sites.** As noted above, *Pvu*I proved to be very useful in constructing the *Bgl*II-*Xba*I restriction map because it selectively cleaved *Bgl*II-2a and -8b so that these fragments could be separated from *Bgl*II-2b and -8a, respectively. No other *Bgl*II fragments were cleaved by *Pvu*I, with the result that digestion with both *Bgl*II and *Pvu*I yielded a set of 17 fragments, only two pairs of which were not well resolved from one another on an agarose gel (Fig. 5). These were *Bgl*II-7a and -7b, which are contiguous on the map, and *Pvu*I-3a and -3b, which also proved to be neighboring fragments.

When T4 dC-DNA was digested with *Pvu*I alone, two small fragments of apparently equal size (*Pvu*I-3a and -3b) were produced along with two very large fragments (Fig. 5). The evidence for two small fragments in *Pvu*I-3 came directly from densitometer tracings of photographic negatives of the gels. The increased density of the *Pvu*I-3 band compared with bands with single fragments of similar size was readily apparent in double digests of *Pvu*I with *Bgl*II or *Xba*I (Fig. 5). The four *Pvu*I cleavage sites were mapped by examining the subfragments produced by *Pvu*I digestion of the individual *Bgl*II and *Xba*I fragments which contained *Pvu*I cleavage sites. The subfragments are identified in Fig. 5 among the products of the double digestion of the T4 *alc* mutant dC-DNA with *Pvu*I and *Bgl*II or *Xba*I. In all cases, only one fit for the *Pvu*I

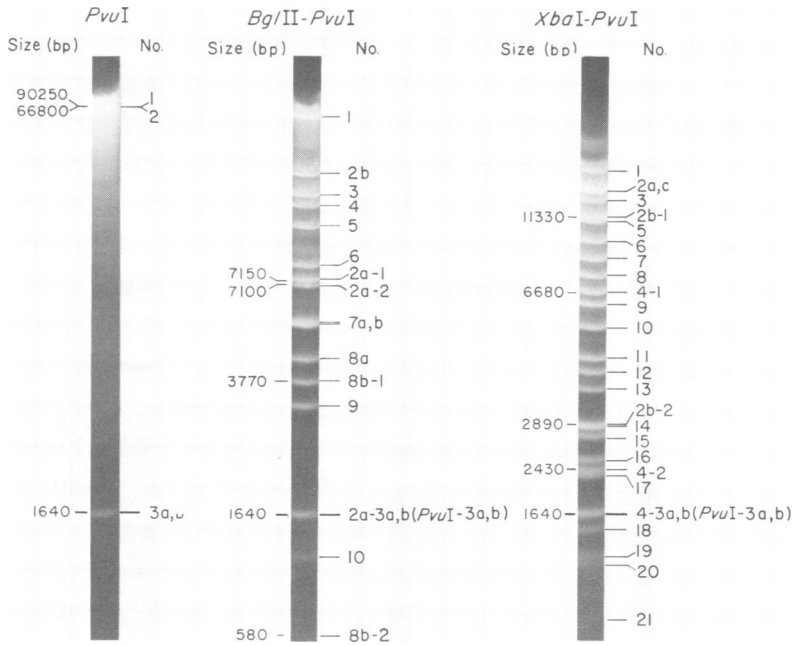


FIG. 5. *Agarose gel electrophoresis of restriction fragments produced by cleavage of T4 alc mutant dC-DNA with PvuI alone and with PvuI in combination with BglII and XbaI. Fragment sizes were determined and subfragments were numbered as described in the legends to Fig. 1 and 3.*

subfragments on the existing *Bgl*II-*Xba*I map was possible, yielding the map of *Pvu*I sites shown in Fig. 2.

In Fig. 5, as in the previous figures, the listed sizes of fragments are adjusted values, which were calculated during construction of the unified restriction map. As described below, these sizes varied only slightly from the original measurements, upon which the actual order of the fragments on the map was based. In the case of the *Pvu*I sites in *Bgl*II-2a, the original measurements for the four *Pvu*I subfragments of *Bgl*II-2a were 7.17, 6.92, 1.64, and 1.64 kb, for a total of 17.4 kb. This compares with the measured size of 17.6 kb for *Bgl*II-2a and an adjusted size of 17.5 kb, corroborating the inclusion of both of the 1.64-kb *Pvu*I-3 fragments within *Bgl*II-2a.

To locate the single *Bam*HI cleavage site (20, 22) on the map, the T4 dC-DNA was digested with both *Bam*HI and *Bgl*II or *Bam*HI and *Xba*I (Fig. 6). As Fig. 6 shows, a 10,440-bp terminal fragment was cleaved from *Bgl*II-1 by *Bam*HI, and *Xba*I-5 was cleaved into 5,780- and 5,210-bp fragments. This uniquely defined the *Bam*HI site as 5,780 bp from the end of *Xba*I-5 proximal to *Xba*I-9, as shown in Fig. 2.

**Map coordinates for the restriction sites.** In the accompanying report (24), the *Bgl*II restriction map was aligned with the T4 genetic map, and the 5.8-kb *r*IIH23B deletion carried by the *alc* quadruple mutant was located within *Bgl*II-4 by DNA heteroduplex mapping. In Fig. 2, the position of the *r*IIH23B deletion is shown, and map coordinates are assigned to the restriction cleavage sites by following the convention of initiating measurement on the genome between the *r*IIA and *r*IIB cistrons and proceeding clockwise. A coordinate of 2,300 bp was used for the left end of the *r*IIH23B deletion, based on the fact that the deletion terminates at the end of the *r*IIA cistron, which has been estimated to contain 2,300 bp by electron microscopy of heteroduplexes formed with various *r*II deletion mutants (8). This value is also in line with estimates based on the molecular weight of the *r*IIA protein (13). Note that the map coordinates in Fig. 2 are the coordinates expected for wild-type T4 DNA with an estimated 166,200 bp per genome, although the restriction maps on the inner circles are for the T4 *alc* quadruple-mutant DNA.

Map coordinates of the cleavage sites were calculated with the computer mapping program of Schroeder and Blattner (15) and the lengths measured by agarose gel electrophoresis for fragments less than 20 kb long. A total of 118 fragment lengths were measured from digests of the T4 *alc* DNA made with *Bgl*II, *Xba*I, *Sal*I, *Kpn*I, *Pvu*I, and *Bam*HI individually and in all pairwise combinations. Maximum agreement be-

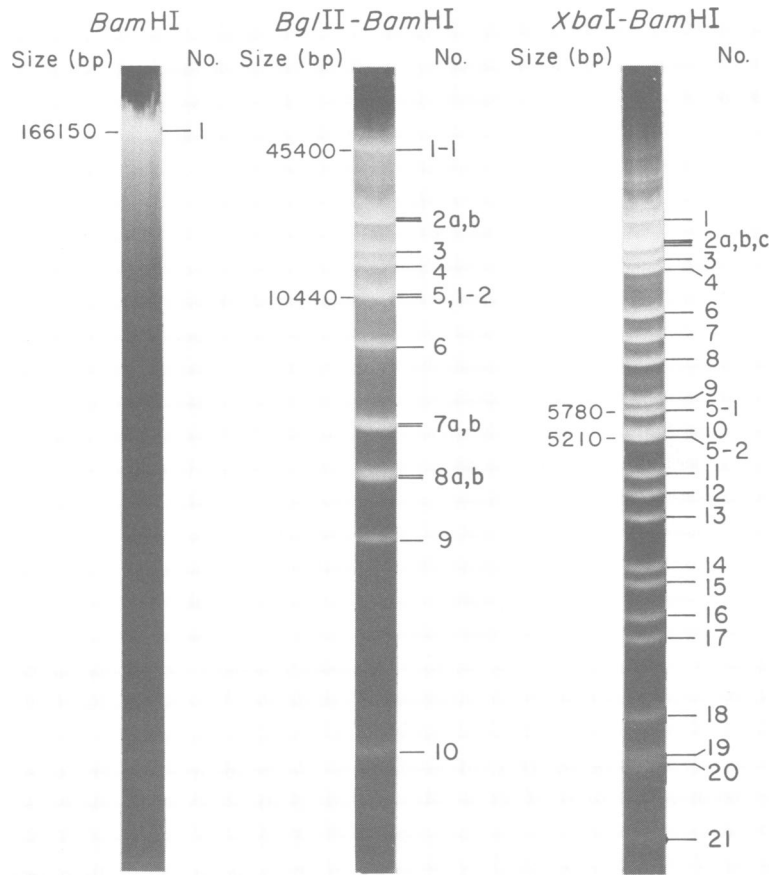


FIG. 6. *Agarose gel electrophoresis of restriction fragments produced by cleavage of T4 alc mutant dC-DNA with BamHI alone and with BamHI in combination with BglII and XbaI. Fragment sizes were determined and subfragments were numbered as described in the legends to Fig. 1 and 3.*

tween the measured fragment sizes and their sizes estimated from the sums of their subfragments and from their contributions to the sizes of longer fragments was achieved by minimizing the sum of the squares of the fractional deviations between the measured and estimated fragment sizes. We used fractional deviations, rather than absolute deviations, since measurement errors with agarose gels increase in direct proportion to fragment length.

Table 2 lists the average measured sizes and computed sizes of the fragments obtained with the individual restriction endonucleases. Measurements were quite reproducible from gel to gel; the standard deviation of the four to six measurements made was less than 3% for all fragments. The computer fit adjusted the measured lengths for all fragments, including those from double digestions not listed in Table 2, by an average of 0.8%. There was no skew in the adjustment with respect to fragment size. The greatest adjustment was 3.0%, for the 14,910-bp subfragment cleaved from *Xba*I-1 by *Kpn*I. Unless otherwise noted, throughout this report we use these adjusted values, which represent an increase in accuracy over the measured values from agarose gels.

Although the map coordinates in Fig. 2 have been reported to 10 bp, this does not reflect the accuracy of each coordinate. Instead, it is the accuracy of the difference between nearby coordinates that should be considered.

## DISCUSSION

The unified restriction map presented here contains 56 recognition sites for the six enzymes *Bam*HI, *Bgl*II, *Kpn*I, *Pvu*I, *Sal*I, and *Xba*I. Its circularity is the result of the permutation in base sequence that is present within a population of mature, linear chromosomes of T4 (21). This permutation arises when concatemers of T4 DNA are cut at random along the base

TABLE 2. *Measured fragment sizes*[a]

| Fragment | Measured size (bp) | Computed size (bp) | % Change | Fragment | Measured size (bp) | Computed size (bp) | % Change |
|---|---|---|---|---|---|---|---|
| *Bam*HI-1 | | 166,150 | | *Sal*I-2b | | 30,640 | |
| | | | | *Sal*I-3 | | 23,630 | |
| *Bgl*II-1 | | 55,840 | | *Sal*I-4 | 15,050 | 15,160 | 0.7 |
| *Bgl*II-2a | 17,580 | 17,530 | −0.3 | *Sal*I-5 | 9,050 | 9,030 | −0.2 |
| *Bgl*II-2b | 17,580 | 17,500 | −0.5 | *Sal*I-6 | 7,140 | 7,110 | −0.8 |
| *Bgl*II-3 | 14,020 | 14,010 | 0 | *Sal*I-7 | 4,140 | 4,150 | 0.2 |
| *Bgl*II-4 | 12,580 | 12,660 | 0.6 | | | | |
| *Bgl*II-5 | 10,380 | 10,580 | 1.9 | *Xba*I-1 | 17,730 | 17,910 | 1.0 |
| *Bgl*II-6 | 7,870 | 7,940 | 0.9 | *Xba*I-2a | 14,470 | 14,530 | 0.4 |
| *Bgl*II-7a | 5,440 | 5,540 | 1.8 | *Xba*I-2b | 14,470 | 14,270 | −1.4 |
| *Bgl*II-7b | 5,440 | 5,470 | 0.6 | *Xba*I-2c | 14,470 | 14,250 | −1.6 |
| *Bgl*II-8a | 4,420 | 4,410 | −0.2 | *Xba*I-3 | 13,180 | 13,150 | −0.2 |
| *Bgl*II-8b | 4,390 | 4,350 | −0.9 | *Xba*I-4 | 12,330 | 12,200 | −1.1 |
| *Bgl*II-9 | 3,330 | 3,330 | 0 | *Xba*I-5 | 10,980 | 11,000 | 0.1 |
| *Bgl*II-10 | 1,180 | 1,180 | 0 | *Xba*I-6 | 9,390 | 9,430 | 0.4 |
| | | | | *Xba*I-7 | 8,240 | 8,090 | −1.8 |
| *Kpn*I-1 | | 46,370 | | *Xba*I-8 | 7,350 | 7,280 | −1.0 |
| *Kpn*I-2 | | 39,380 | | *Xba*I-9 | 6,150 | 6,180 | 0.5 |
| *Kpn*I-3 | | 36,730 | | *Xba*I-10 | 5,330 | 5,210 | −2.2 |
| *Kpn*I-4 | | 24,190 | | *Xba*I-11 | 4,390 | 4,450 | 1.4 |
| *Kpn*I-5 | 8,940 | 8,890 | −0.6 | *Xba*I-12 | 4,080 | 4,090 | 0.2 |
| *Kpn*I-6 | 3,330 | 3,330 | 0 | *Xba*I-13 | 3,670 | 3,640 | −0.8 |
| *Kpn*I-7 | 1,450 | 1,450 | 0 | *Xba*I-14 | 2,970 | 2,890 | −2.7 |
| | | | | *Xba*I-15 | 2,790 | 2,790 | 0 |
| *Pvu*I-1 | | 90,250 | | *Xba*I-16 | 2.420 | 2,430 | 0.4 |
| *Pvu*I-2 | | 66,800 | | *Xba*I-17 | 2,150 | 2,150 | 0 |
| *Pvu*I-3a | 1,640 | 1,640 | 0 | *Xba*I-18 | 1,450 | 1,450 | 0 |
| *Pvu*I-3b | 1,640 | 1,640 | 0 | *Xba*I-19 | 1,180 | 1,180 | 0 |
| | | | | *Xba*I-20 | 1,110 | 1,110 | 0 |
| *Sal*I-1 | | 38,760 | | *Xba*I-21 | 680 | 680 | 0 |
| *Sal*I-2a | | 31,870 | | | | | |

[a] This table shows lengths of fragments as measured by agarose gel electrophoresis and as adjusted by computation during construction of the unified restriction map (Fig. 2). Also shown is the percent difference in the two values. Sizes were not measured directly from agarose gels for fragments more than 20 kb long. The reported sizes of these fragments represent the sums of their adjusted subfragment lengths.

sequence for packaging into phage heads (11, 17).

The map coordinates determined for the 56 sites represent a best fit of the length measurements made on 118 fragments from single and double enzyme digestions and are based on a least-squares analysis. Other workers have constructed maps of the cleavage sites for several of the same enzymes. A map of the *Kpn*I and *Sal*I sites was reported by Carlson and Nicolaisen (3), and maps for these enzymes plus *Bam*HI and *Bgl*II were reported by Rüger and co-workers (7, 14) and by O'Farrell et al. (13). Our map adds the 27 sites cleaved by *Pvu*I and *Xba*I and identifies the coordinates for the cleavage sites of all six enzymes with a precision not previously available.

Our map confirms the finding by Rüger et al. (14) that their first reported map (7) contained two neighboring *Bgl*II fragments and three *Kpn*I fragments inverted with respect to the rest of the map. By our nomenclature, these were *Bgl*II fragments 2a and 3 and *Kpn*I fragments 3, 5, and 7. Also confirmed is the presence of *Kpn*I fragment 6, which was absent on the map of Carlson and Nicolaisen (3) but present on the map of Kiko et al. (7). Carlson (2) has now found that this *Kpn*I fragment is also present in digests from the T4 strain which she used for mapping. Thus, the number and relative position of each of the *Bgl*II and *Kpn*I cleavage sites are in total agreement for the T4 strains mapped in these laboratories and in our laboratory. The maps of the *Sal*I and *Bam*HI cleavage sites are also in agreement.

The T4 *alc* mutant which we used carries an extensive deletion, which covers the *r*II cistrons and extends to the *ac* gene. Some *Bgl*II, *Kpn*I, *Pvu*I, and *Xba*I sites may occur in this region and, therefore, be missing from the map. It is known that one *Sal*I cleavage site falls within the deleted region, but it contains no *Bam*HI cleavage sites (13, 20).

Cleavage of T4 DNA by *Pvu*I and *Xba*I should

be especially useful for further genetic and biochemical studies. The arrangement of the *Pvu*I cleavage sites, with three equidistant sites clustered on one side of the genome and opposite the fourth site, effectively divides the genome in half. With *Xba*I, the resulting fragments are moderate in size and, except for three that overlap, are well resolved as individual bands by electrophoresis in agarose gels. Since no other single restriction endonuclease or combination of enzymes is known to resolve the T4 genome so well in one step, *Xba*I should facilitate Southern blot hybridization analyses.

An alignment of the *Xba*I cleavage map with the T4 genetic map is described in the accompanying paper (24). It is of interest that *Xba*I cleaves five times within the relatively genetically silent 15-kb region between genes 55 and *r*I. Few other restriction sites have been located in this region (12).

The sum of adjusted fragment lengths yields a genome of 160,350 bp for the T4 *alc* mutant which we studied. With the addition of the 5.8-kb *r*IIH23B deletion, the wild-type T4 genome contains 166,200 bp. A similar genome size of 166 ± 2 kb was determined previously by Kim and Davidson (8), based on measurements of T4 DNA molecules and T2/T4 heteroduplex molecules visualized by electron microscopy. This close agreement on the genome size is somewhat fortuitous, however, as the length of the phage λ DNA used as a standard by Kim and Davidson has since been revised upward by about 5% (4).

The mature, linear chromosome of T4 carries a 3.3- ± 1-kb terminal redundancy (8). Given this additional DNA, our measurements yield a chromosome size of 169,500 bp.

## ACKNOWLEDGMENTS

We thank Louis Wadel for assistance in adapting the mapping program of Schroeder and Blattner (15) to our computer facilities.

This investigation was supported by Public Health Service research grant GM 23608 from the National Institute of General Medical Sciences and by Public Health Service Research Career Development Award CA 00490 to R.C.M. from the National Cancer Institute.

## LITERATURE CITED

1. **Blin, N., A. V. Gabain, and H. Bujard.** 1975. Isolation of large molecular weight DNA from agarose gels for further digestion by restriction enzymes. FEBS Lett. **53**:84–86.
2. **Carlson, K.** 1980. Correlation between genetic map and map of cleavage sites for sequence-specific endonucleases *Sal*I, *Kpn*I, *Bgl*I, and *Bam*HI in bacteriophage T4 cytosine-containing DNA. J. Virol. **36**:1–17.
3. **Carlson, K., and B. Nicolaisen.** 1979. Cleavage map of bacteriophage T4 cytosine-containing DNA by sequence-specific endonucleases *Sal*I and *Kpn*I. J. Virol. **31**:112–123.
4. **Daniels, D. L., J. R. de Wet, and F. R. Blattner.** 1980. New map of bacteriophage lambda DNA. J. Virol. **33**: 390–400.
5. **Georgopoulos, C. P., and H. R. Revel.** 1971. Studies with glycosyl transferase mutants of the T-even bacteriophage. Virology **44**:271–285.
6. **Kaplan, D. A., and D. P. Nierlich.** 1975. Cleavage of nonglucosylated bacteriophage T4 deoxyribonucleic acid by restriction endonuclease *Eco* RI. J. Biol. Chem. **250**:2395–2397.
7. **Kiko, H., E. Niggemann, and W. Rüger.** 1979. Physical mapping of the restriction fragments obtained from bacteriophage T4 dC-DNA with restriction endonucleases *Sma*I, *Kpn*I and *Bgl*II. Mol. Gen. Genet. **172**:303–312.
8. **Kim, J.-S., and N. Davidson.** 1974. Electron microscope heteroduplex study of sequence relations of T2, T4, and T6 bacteriophage DNAs. Virology **57**:93–111.
9. **Kutter, E., A. Beug, R. Sluss, L. Jensen, and D. Bradley.** 1975. The production of undegraded cytosine-containing DNA by bacteriophage T4 in the absence of dCTPase and endonucleases II and IV, and its effect on T4-directed protein synthesis. J. Mol. Biol. **99**:591–607.
10. **Lawn, R., E. Fritsch, R. Parker, G. Blake, and T. Maniatis.** 1978. The isolation and characterization of linked δ- and β-globin genes from a cloned library of human DNA. Cell **15**:1157–1174.
11. **Mosig, G., J. Renshaw-Carnighan, J. Baxandall-Bibring, R. Cole, H. O. Bock, and S. Bock.** 1972. Coordinate variation in lengths of deoxyribonucleic acid molecules and head lengths in morphological variants of bacteriophage T4. J. Virol. **9**:857–871.
12. **O'Farrell, P., E. Kutter, and M. Nakanishi.** 1980. A restriction map of the bacteriophage T4 genome. Mol. Gen. Genet. **179**:421–435.
13. **O'Farrell, P. Z., L. M. Gold, and W. M. Huang.** 1973. The identification of prereplicative bacteriophage T4 proteins. J. Biol. Chem. **248**:5499–5501.
14. **Rüger, W., M. Neumann, U. Rohr, and E. Niggemann.** 1979. The complete maps of *Bgl*II, *Sal*I and *Xho*I restriction sites on T4 dC-DNA. Mol. Gen. Genet. **176**: 417–425.
15. **Schroeder, J. L., and F. R. Blattner.** 1978. Least-squares method for restriction mapping. Gene **4**:167–174.
16. **Snyder, L., L. Gold, and E. Kutter.** 1976. A gene of bacteriophage T4 whose product prevents true late transcription on cytosine-containing T4 DNA. Proc. Natl. Acad. Sci. U.S.A. **73**:3098–3102.
17. **Streisinger, G., J. Emrich, and M. M. Stahl.** 1967. Chromosome structure in phage T4. III. Terminal redundancy and length determination. Proc. Natl. Acad. Sci. U.S.A. **57**:292–295.
18. **Sugden, B., B. DeTroy, R. J. Roberts, and J. Sambrook.** 1975. Agarose slab-gel electrophoresis equipment. Anal. Biochem. **68**:36–46.
19. **Sutcliffe, J. G.** 1978. pBR322 restriction map derived from the DNA sequence: accurate DNA size markers up to 4361 nucleotide pairs long. Nucleic Acids Res. **5**: 2721–2728.
20. **Takahashi, H., M. Shimizu, H. Saito, and Y. Ikeda.** 1979. Studies of viable T4 bacteriophage containing cytosine-substituted DNA (T4dC phage). II. Cleavage of T4dC DNA by endonucleases *Sal*I and *Bam*HI. Mol. Gen. Genet. **168**:49–53.
21. **Thomas, C. A., Jr., and L. A. MacHattie.** 1964. Circular T2 DNA molecules. Proc. Natl. Acad. Sci. U.S.A. **52**: 1297–1301.
22. **Wilson, G. G., R. L. Neve, G.J. Edlin, and W. H. Konigsberg.** 1979. The *Bam* H1 restriction site in the bacteriophage T4 chromosome is located in or near gene 8. Genetics **93**:285–296.
23. **Wood, W. B., and H. R. Revel.** 1976. The genome of bacteriophage T4. Bacteriol. Rev. **40**:847–868.
24. **Yee, J. K., and R. C. Marsh.** 1981. Alignment of a restriction map with the genetic map of bacteriophage T4. J. Virol. **38**:115–124.